Fe and Mo EXAFS of *Azotobacter vinelandii* Nitrogenase in Partially Oxidized and Singly Reduced Forms

J. Christiansen,[†] R. C. Tittsworth,[‡] B. J. Hales,[‡] and S. P. Cramer*,[†,§]

Contribution from the Department of Applied Science, University of California, Davis, California 95616, Department of Chemistry, Louisiana State University, Baton Rouge, Louisiana 70803, and Energy and Environment Division, Lawrence Berkeley Lab, Berkeley, California 94720

Received May 22, 1995[⊗]

Abstract: Fe and Mo K-edge EXAFS spectra of the nitrogenase MoFe protein in the indigo disulfonate (IDS) oxidized form and under slow turnover conditions have been recorded. The EXAFS of the one-electron reduced form E_1 was obtained as a difference spectrum between the slow turnover and resting (E_0) spectra. Average Fe−S, Fe−Fe, and Fe−Mo distances of 2.33, 2.60, and 2.66 Å, respectively, along with a second Fe−Fe distance at 3.72 Å were found for E_1. The IDS-oxidized MoFe protein contains partially oxidized "P-clusters". For this sample, average Fe−S, Fe−Fe, and Fe−Mo interactions at 2.31, 2.65, and 2.71 Å, respectively, were found along with the long Fe−Fe interaction at 3.74 Å. Combination of the current results with previous data on resting and thionin-oxidized nitrogenase shows a general trend—a significant number of the metal−metal distances tend to contract as the enzyme becomes more reduced.

Introduction

The enzyme nitrogenase catalyzes the reduction of dinitrogen to ammonia, along with hydrogen evolution and ATP hydrolysis.[1−3] X-ray crystallography has shown that the nitrogenase MoFe protein is an $\alpha_2\beta_2$ tetramer with two unique types of metal clusters.[4] One of these, the "P-cluster", is proposed to consist of two [Fe_4S_4] clusters bridged by two cysteinyl sulfurs and a disulfide bond formed between two of the cluster sulfurs,[5] although another crystallographic model has been proposed which links the two cubes at a single sulfur.[6] The other cluster can be viewed as a [$MoFe_3S_3$] fragment bridged by three inorganic sulfides to another [Fe_4S_3] cluster (Figure 1).[4,6] This cluster, first spectroscopically identified as the "M-center",[7] is thought to be the site of enzymatic activity, and it is extractable as the [$MoFe_7S_9$ + homocitrate] "FeMo-cofactor".[8]

Along with valuable magnetic resonance and Mössbauer studies,[1−3,7] there have been numerous EXAFS studies of MoFe protein solutions,[9] crystals,[10] and extracted FeMo-cofactor.[11] Since there is only one type of Mo present, the Mo EXAFS has been relatively easy to interpret, and components corresponding to Mo−O,N, Mo−S, and Mo−Fe interactions at ~2.1, 2.4, 2.7 Å have been reported and assigned (Figure 1). On the other hand, the Fe EXAFS of the nitrogenase MoFe protein is complicated by the presence of 15 different types of Fe distributed over two metal clusters. The Fe EXAFS of intact nitrogenase yielded average Fe−S, Fe−Fe, and Fe−Mo distances of 2.29, 2.62, and 2.74 Å as well as a long Fe−Fe interaction of 3.75 Å. Combination of the Fe and Mo EXAFS data with the crystallographic results recently allowed refinement of a model for the M center.[9]

Despite rapid progress in characterization of the resting nitrogenase system, there is no crystallographic information on the cluster structures once electrons are put into the M center. One obstacle to characterization of the reduced enzyme is H_2 evolution by the two-electron reduced form E_2, which returns the reduced enzyme back to the resting state E_0.[12] The E_1 form may also be capable of reverting to E_0 via oxidation by sulfite.[13] Information about the reduced structures is important, because most substrates or inhibitors bind only after electrons are added to the M center.[1,8] For example, irreversible dinitrogen binding is proposed to occur at the E_3 reduction level.[12] In this current paper, we use EXAFS to examine how the average Fe−X and Mo−X distances change upon reduction to E_1, and we also investigate change with P-cluster or M-center oxidation.

Experimental Section

Sample Preparation. Nitrogenase MoFe protein was extracted from strains of *Azotobacter vinelandii* and purified by previously published methods.[14] Specific activities of purified enzyme ranged from 1800−2000 nmol C_2H_2 reduced min^{-1} mg $protein^{-1}$ for the MoFe protein and 1400−1600 nmol C_2H_2 reduced min^{-1} mg $protein^{-1}$ for the Fe protein. All purification steps were done under strictly anaerobic

[†] University of California.
[‡] Louisiana State University.
[§] Lawrence Berkeley Lab.
[⊗] Abstract published in *Advance ACS Abstracts,* September 1, 1995.

(1) Orme-Johnson, W. H. *Annu. Rev. Biophys. Biophys. Chem.* **1985**, *14*, 419−459.
(2) Eady, R. R. *Adv. Inorg. Chem.* **1991**, *36*, 77−102.
(3) Hageman, R. V.; Burris, R. H. *Proc. Natl. Acad. Sci. U. S. A.* **1978**, *75*, 2699−2702.
(4) Kim, J. C.; Rees, D. C. *Science* **1992**, *257*, 1677.
(5) Chan, M. K.; Kim, J.; Rees, D. C. *Science* **1993**, *260*, 792−794.
(6) Campobasso, N. Ph.D. Thesis, Purdue University, 1994.
(7) Zimmerman, R.; Munck, E.; Brill, W. J.; Shah, V. K.; Henzl, M. T.; Rawlings, J.; Orme-Johnson, W. H. *Biochim. Biophys. Acta* **1978**, *537*, 185−207.
(8) Burgess, B. K. *Chem. Rev.* **1990**, *90*, 1377−1406.
(9) Chen, J.; Christiansen, J.; Tittsworth, R. C.; Hales, B. J.; George, S. J.; Coucouvanis, D.; Cramer, S. P. *J. Am. Chem. Soc.* **1993**, *115*, 5509−5515 and references cited therein.
(10) (a) Flank, A. M.; Weininger, M.; Mortenson, L. E.; Cramer, S. P. *J. Am. Chem. Soc.* **1986**, *108*, 1049−1055. (b) Chen, J.; Christiansen, J.; Campobasso, N.; Bolin, J. T.; Tittsworth, R. C.; Hales, B. J.; Rehr, J. J.; Cramer, S. P. *Angew. Chem., Int. Ed. Engl.* **1993**, *32*, 1592−1594.
(11) (a) Conradson, S. D.; Burgess, B. K.; Newton, W. E.; Mortenson, L. E.; Hodgson, K. O. *J. Am. Chem. Soc.* **1987**, *109*, 7507. (b) Arber, J. M.; Flood, A. C.; Garner, C. D.; Gormal, C. A.; Hasnain, S. S.; Smith, B. E.; *Biochem. J.* **1988**, *252*, 421−425. (c) Antonio, M. R.; Teo, B. K.; Orme-Johnson, W. H.; Nelson, M. J. Groh, S. E.; Lindahl, P. A.; Kauzlaurich, S. M.; Averill, B. A. *J. Am. Chem. Soc.* **1986**, *108*, 1049−1055.
(12) Lowe, D. J.; Thorneley, R. N. F. *Biochem. J.* **1984**, *224*, 877−886.
(13) Henzl, M. T. Ph.D. Thesis, University of Wisconsin, 1980.
(14) Burgess, B. K.; Jacobs, D. B.; Stiefel, E. I. *Biochim. Biophys. Acta* **1980**, *814*, 198−209.

0002-7863/95/1517-10017$09.00/0

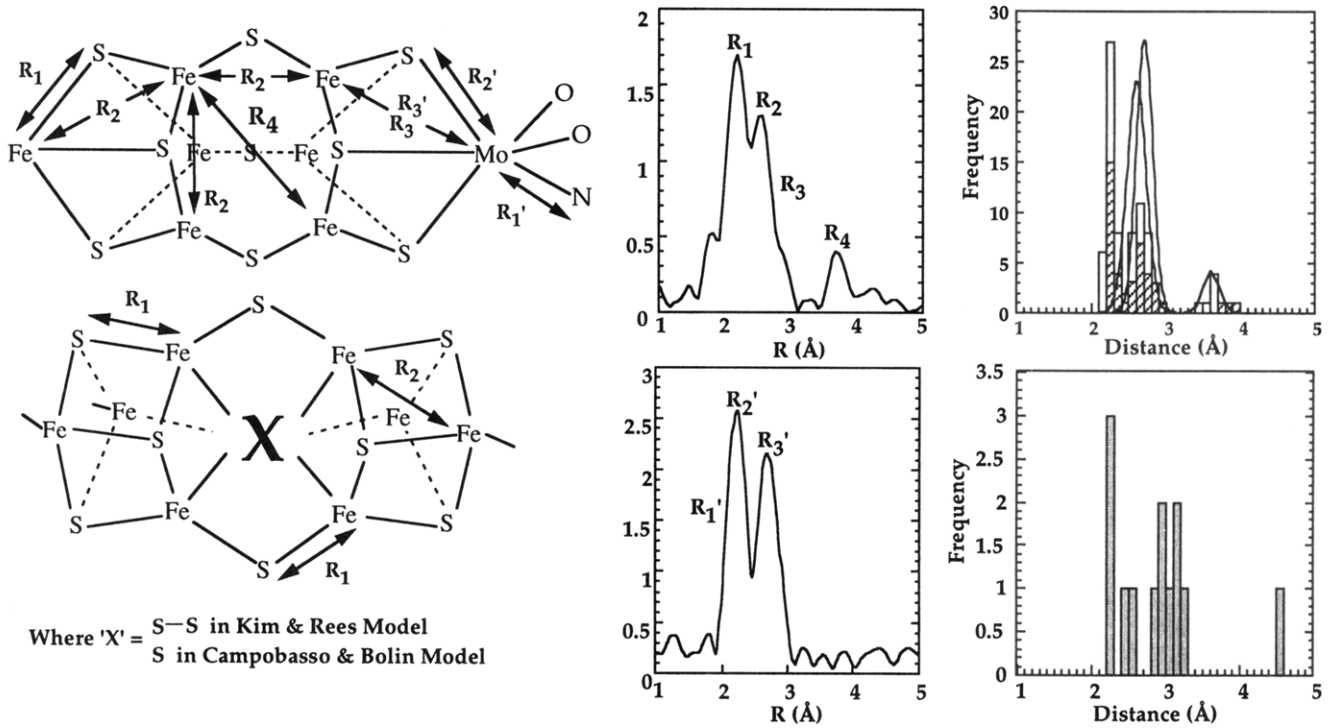

Figure 1. (left) Proposed models for the FeMo-cofactor and P-cluster with some representative distances derived from EXAFS. The accompanying Fourier transforms for the Fe K-edge (top, center) and Mo K-edge (bottom, center) have labels that show the correspondence between the Fourier transform features and the distances shown on the models. The histograms were derived from recent crystallographic coordinates[6] and correspond to interactions from Fe (top, right) and Mo (bottom, right). The Gaussian curves shown on the Fe histogram represent the spread in similar Fe−Fe distances in the P-cluster and M-center.

conditions. Purified fractions were stored frozen in liquid nitrogen. Protein concentration was determined by the biuret method.

To obtain a pure one-electron reduced spectrum, we examined a steady-state mixture of resting and one-electron reduced MoFe protein from *Azotobacter vinelandii*, in the presence of a small amount of Fe protein. Under these conditions, almost all protein in the two-electron reduced state E_2, by the scheme of Lowe and Thorneley,[12,15] will rapidly evolve hydrogen and be oxidized back to the resting state, E_0. Thus, a steady-state sample of nearly 50% E_0 and 50% E_1 states can be obtained that has a negligible background contribution from the Fe protein. We measured the Fe K-edge EXAFS of these $E_0 + E_1$ steady-state samples and subtracted the 50% E_0 contribution, thus isolating an E_1 spectrum. Specifically, steady-state mixtures were prepared by incubating a 5:1 molar ratio of MoFe protein:Fe protein, along with excess sodium dithionite and an ATP regenerating mixture at room temperature in a vacuum atmospheres glovebox with an argon atmosphere. The O_2 level was held at <1.5 ppm throughout the entire procedure. The regenerating mixture consisted of 0.025 M Tris-HCl pH 7.4, with 10 mM sodium dithionite, 10 mM Mg-ATP, 150 mM creatine phosphate, and 0.625 mM creatine phosphokinase. Purified MoFe protein was added to the reaction mixture first, followed by the Fe protein to start the reaction. The reaction was allowed to proceed in the glovebox for 8 min, at which time ethylene glycol (as a glassing agent) was added to the reaction mixture, for a final concentration of 40% ethylene glycol, and 20 mg/mL MoFe protein. The reduced samples were loaded into lucite EXAFS cuvettes and quartz EPR tubes simultaneously. The samples were then frozen, typically at 15 min from the point of addition of the Fe protein.

The sample condition was verified by EPR spectroscopy. Steady-state mixture samples all showed 50 ± 2.5% reduction in the amplitude of the $S = 3/2$ FeMo-cofactor signal compared to the control samples in spectra recorded at 3.2 K. EPR spectra were recorded on a computer-interfaced Bruker ER300D spectrometer with ESP 200 data collection software and an Oxford Instruments ESR-900 helium flow cryostat. Temperature was monitored with an FeAu/Chromel thermocouple positioned directly below the sample tube and monitored with an Oxford Instruments ITC-4 temperature controller.

(15) Fisher, K.; Lowe, D. J.; Thorneley, R. N. F. *Biochem. J.* **1991**, *279*, 81−85.

MoFe protein with oxidized P-clusters was prepared by oxidation with indigodisulfonate (IDS).[16] EPR spectroscopy has shown that the $S = 3/2$ signal attributed to the FeMo-cofactor resting state persists,[17] while signals that are attributed to P-cluster oxidation appear.[18] P-cluster oxidation by IDS was effected by titrating dithionite-free MoFe protein with anaerobic IDS solution prepared in 0.025 M Tris-HCl pH 7.4 and 0.2 M NaCl. The titration proceeded until the endpoint was indicated by a persistent blue-green color. Sodium dithionite was removed from the MoFe protein by gel filtration with Sephadex G-25 (Pharmacia), eluting with anaerobic, dithionite-free, 0.026 M Tris-HCl pH 7.4 and 0.2 M NaCl buffer. Eluted MoFe protein fractions were checked for residual dithionite with methyl viologen indicator. IDS oxidized samples were concentrated with Minicon membrane concentrators to a final concentration of 90−140 mg/mL. EXAFS cuvettes and quartz EPR tubes were loaded and frozen in liquid nitrogen simultaneously. All of the above procedures were done in a glovebox with the O_2 level held at <1.5 ppm throughout the entire procedure. EPR spectra showed no attenuation of the $S = 3/2$ FeMo-cofactor signal when compared to untitrated control samples. The $S \geq 3$ signal (at $g = 11.6$ in perpendicular mode) which has been assigned to 2-equivalent oxidized P-clusters was present in IDS oxidized samples.[19] Other EPR signals that are assigned to different P-cluster oxidation states ($S =$ 1/2, 5/2, or 7/2)[18c,19] were not present.

Data Collection. The EXAFS spectra were measured in fluorescence mode using a Canberra Instruments 13-element Ge solid-state

(16) Orme-Johnson, W. H.; Paul, L.; Meade, J.; Warren, W.; Nelson, M.; Groh, S.; Orme-Johnson, N. R.; Munck, E.; Huynh, B. N.; Emptage, M.; Rawlings, J.; Smith, J.; Roberts, J.; Hoffman, B.; Mims, W. B. In *Current Perspectives in Nitrogen Fixation*; Gibson, A. H., Newton, W. E., Eds.; Elsevier: North-Holland, New York, 1981; pp 79−84.

(17) Munck, E.; Rhodes, H.; Orme-Johnson, W. H.; Davis, L. C.; Brill, W. J.; Shah, V. K. *Biochim. Biophys. Acta* **1975**, *400*, 32−53.

(18) (a) Hagen, W. R. In *Iron Sulfur Proteins*. Sykes, A. G., Cammack, R., Eds.; *Advances in Inorganic Chemistry*; Academic Press: New York, 1992; Vol. 38, pp 165−122. (b) Surerus, K. K.; Hendrich, M. P.; Christie, P. D.; Rottgardt, D.; Orme-Johnson, W. H.; Munck, E. J. *J. Am. Chem. Soc.* **1992**, *114*, 8579−8590. (c) Plerik, A. J.; Wassink, H.; Haaker, H.; Hagen, W. R. *Eur. J. Biochem.* **1993**, *212*, 51−61.

(19) Tittsworth, R. C.; Hales, B. J. *J. Am. Chem. Soc.* **1993**, *115*, 9763−9767.

array detector.[20] During the measurement, the samples were maintained at 8−10 K in an Oxford Instruments CF1208 liquid helium flow cryostat. Amplifier shaping times were set at either 0.5 or 1 μs, with total count rates for each channel kept below 35 and 20 kHz, respectively. Single channel analyzer windows were set to collect the Fe or Mo Kα signal. The spectra were calibrated by simultaneously collecting transmission spectra of a pure metal foil, setting the first inflection point energy to be 7111.2 eV for Fe and 20 000 eV for Mo.

X-ray absorption spectra were recorded on several different beamlines. Steady-state turnover MoFe protein Fe XAS data was collected on NSLS beamline X-10C, running in focused mode with Si(220) and Si(111) monochromator configurations; SSRL beamline 6-2 in focused mode and Si(111) monochromator configuration; and NSLS beamline X-19A, in unfocused mode with Si(220) monochromator configuration. IDS oxidized data was collected on NSLS beamline X-19A, in unfocused mode with a Si(111) monochromator configuration; NSLS beamline X-10C, running in focused mode with a Si(111) monochromator configuration; SSRL beamline 6-2, focused mode with a Si-(111) monochromator configuration. For beamlines X-19A and 6-2, the second monochromator crystal was detuned to minimize the transmission of harmonics. For beamline X-10C, a mirror feedback system was used for rejection of harmonics.[21] Beam spot size was maintained at a maximum of ~2 × 12 mm with focusing optics and/or tantalum slits placed at the beam exit port. The incident beam intensity was monitored with a nitrogen-filled ion chamber. Mo X-ray absorption spectra were recorded at SSRL beamline 7-3, operating in unfocused mode with a Si(220) monochromator, and at NSLS beamline X19A, in unfocused mode with a Si(220) monochromator. For Mo samples, the beam intensity was monitored with argon filled ion chambers, and the spot size was maintained by slits placed at the beam exit port.

Analysis Procedures. The use of different beamlines and monochromator crystals helped reduce systematic experimental errors associated with monochromator glitches and the overall spectral baseline. Reproducibility was checked by overlaying the data sets and comparing the EXAFS over the full range of data. The individual scans were deglitched, if necessary, using single point removal. All deglitching was performed prior to isolation of the EXAFS oscillations, so as not to induce any spline errors. The EXAFS oscillations were extracted from the raw data with a cubic spline and normalized with a Victoreen function using routine methods.[22] E_0 values of 7131 eV for Fe and 20 020 eV for Mo were used to initially define the magnitude of the photoelectron wave vector $k = [(8\pi^2 m/h^2)(E - E_0)]^{1/2}$. The EXAFS spectra were interpolated onto identical k-space grids with $\Delta k = 0.05$ Å^{-1} and then averaged to form a single data set for both the singly reduced mixture ($E_0 + E_1$) and IDS oxidized MoFe protein. The EXAFS spectrum of resting E_0 MoFe protein was also interpolated onto the same k-space grid and subtracted from the $E_0 + E_1$ mixture to yield the EXAFS of the E_1 state.

The EXAFS spectra were Fourier transformed from k-space to R-space, and specific regions of the resulting transforms were then Fourier filtered and back-transformed as will be described later. The resulting filtered EXAFS spectra were then fit to the single-scattering, curved-wave functional form of the EXAFS equation[23] using the McKale functions and a Levenberg−Marquardt curve fitting algorithm[24]

$$\chi(k) = \sum_i \frac{N_i \gamma_i f_i(k,R_i)}{kR_i^2} e^{-2\sigma_i^2 k^2} \sin[2kR_i + \phi_i(k,R_i)]$$

where the summation is over all backscatterers at a distance R_i, with root-mean square distance deviation σ_i^2; and coordination number N_i. The functions $f(k,R_i)$ and $\phi(k,R_i)$[23] represent the distance and energy dependent, curved-wave backscattering amplitude and total phase shift, respectively. The amplitude reduction factor, γ, was held fixed at 0.9 during all fits.[9]

Appropriate values for the threshold energy shifts ΔE_0 for Fe−X and Mo−X interactions were derived by fitting spectra of the model compounds $[Fe_6S_6Cl_6]^{3-}$ and $(CO)_3MoFe_6S_6Mo(CO)_3$[9,25] with theoretical phase shift and amplitude functions, while constraining the distances to crystallographic values. For the $(CO)_3MoFe_6S_6Mo(CO)_3$ model, multiple scattering was taken into account for the relevant Mo−CO interactions. Parameters taken from model compound fit results were held fixed for all fits. The appropriate values for coordination numbers N were derived from inspection of the crystallographic models.[4−6] The values for the distance R and distance deviation σ^2 were allowed to vary, with published results being used as initial values for these parameters.[9,10] For all Fe K-edge fits, the Fe−Mo interaction was held fixed at the value derived from the Mo K-edge fits, this added another element of self-consistency and reduced the degrees of freedon in the resulting fits. In fits that used the Fe−Mo distance derived from the Fe K-edge fits, the resulting split in the Fe−Fe distances was actually more pronounced.

Results and Discussion

EXAFS Fourier Transforms vs Crystallographic Radial Distributions. In Figure 1, we compare the radial distribution functions around Fe and Mo, derived from a recent crystallographic analysis of the *C. pasteurianum* MoFe protein,[6] with the phase-shift corrected Fe and Mo EXAFS Fourier transforms. In the P cluster, the average short Fe−Fe distance is proposed to be 2.71 Å, with a root mean square deviation σ of 0.11 Å.[6] The crystallographic data suggest that the average M center Fe−Fe distance is a shorter 2.60 Å, with a root mean square deviation σ of 0.13 Å. The current range of EXAFS data does not allow resolution of these two groups of distances, but the "split-shell" distribution can be modeled by curve-fitting. At longer distances, the M center has an important group of "cross-cluster" Fe−Fe interactions at an average distance of 3.61 Å. The single-scattering analysis of these interactions is complicated by multiple-scattering paths that have similar total lengths. However, multiple scattering is not important for the interactions at distances <3 Å.

IDS Oxidized MoFe Protein. The Fe EXAFS Fourier transform of IDS-oxidized MoFe protein (P^{2+}/M) is compared with resting (P/M) and thionin-oxidized (P^{2+}/M^+) protein in Figure 2. Like thionin-oxidized MoFe protein, there is a decrease in the intensity of the ~2.7 Å transform peak, compared to the resting MoFe protein transform. The 3.7 Å peak, first observed in the extracted FeMo-cofactor,[11b] remains of similar magnitude in the IDS data as in the resting enzyme.[9] Since the oxidation state of the M-center is not affected by IDS oxidation, a large change in the M-center distances is not expected. For curve fitting analysis, the Fe EXAFS of the IDS oxidized MoFe protein was Fourier transformed (k = 3−14.5 Å^{-1}), and then the R-space region from 0−6 Å was back-transformed. To limit the number of free parameters in the simulations, the Fe−Mo distance was fixed at the 2.71 Å value obtained from the Mo K-edge EXAFS of resting enzyme. The best four shell single-scattering fit with this constraint (Table 1 and Figure 2), found average Fe−S and Fe−Fe distances of 2.31 and 2.65 Å as well as a long Fe−Fe component at 3.74 Å.

Since the fit to the data is good but not perfect, the significance of multiple scattering in the Fe EXAFS was estimated using the FEFF5 program.[26] For these calculations, a symmetrized model for the core of the M-center was

(20) Cramer, S. P.; Tench, O.; Yocum, M.; George, G. N. *Nucl. Instrum. Methods A266*, **1988**, 586−591.

(21) Sansone, M.; Via, G.; George, G. N.; Meitzner, G.; Hewitt, R. In *X-Ray Absorption Fine Structure*; Hasnain, S. S., Ed.; Ellis Horwood Ltd.: West Sussex, England, 1991; pp 656−658.

(22) Cramer, S. P.; Hodgson, K. O.; Stiefel, E. I.; Newton, W. O. *J. Am. Chem. Soc.* **1978**, *100*, 2478−2760.

(23) McKale, A. G.; Knapp, G. S.; Chan, S.-K. *Phys. Rev. B* **1986**, *33*, 841−846.

(24) Marquardt, D. W. *J. Soc. Ind. Appl. Math.* **1963**, *11*, 443.

(25) Coucouvanis, D.; In *Molybdenum Enzymes, Cofactors and Model Systems*; Stiefel, E. I., Coucouvanis, D., Newton, W. E., Eds.; ACS Symposium Series 535, New York; 1993; pp 304−331.

(26) (a) Rehr, J. J.; Mustre de Leon, J.; Zabinsky, S. I.; Albers, R. C. *J. Am. Chem. Soc.* **1991**, *113*, 5135. (b) Mustre de Leon, J.; Rehr, J. J.; Zabinsky, S. I.; Albers, R. C. *Phys. Rev. B* **1991**, *44*, 4146.

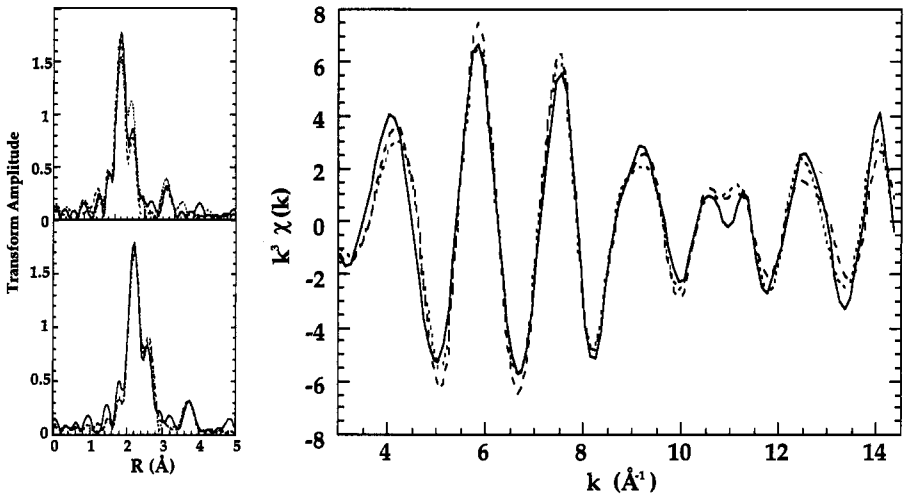

Figure 2. *Left, top:* Fourier transforms (corrected for Fe−Fe phase shift) of IDS oxidized protein (solid) and thionine oxidized (dashed) and resting MoFe protein (dotted). *Left, bottom:* Fourier transforms of IDS oxidized protein with resulting fits. *Right:* Fourier filtered Fe EXAFS of IDS oxidized nitrogenase (solid) shown with the four component (short dash) and unconstrained five component (long dash) fit results.

Table 1. *Azotobacter vinelandii* Nitrogenase Fe K-Edge EXAFS Fitting

	Fe−S[b]			Fe−Fe[c]			Fe−Mo[d]			Fe−Fe′ [e]			
	N	R, Å	$\sigma^2 \times 10^{-5}$, Å^2	N	R, Å	$\sigma^2 \times 10^{-5}$, Å^2	N	R, Å	$\sigma^2 \times 10^{-5}$, Å^2	N	R, Å	$\sigma^2 \times 10^{-5}$, Å^2	F[a]
Thionine Oxidized (P^{2+}/M^{+})													
4 components	3.6	2.29	555	3.2	2.66	988	0.2	2.72	443	1.3	3.73	369	0.46
5 components	3.6	2.29	501	1.6	2.61	333	0.2	2.72	443	1.3	3.74	395	0.56
				1.6	2.74	333							
5 components	3.6	2.29	521	1.6	2.62	430	0.2	2.72	443	1.3	3.73	425	0.41
				1.6	2.73	549							
IDS Oxidized (P^{2+}/M)													
4 components	3.6	2.31	506	3.2	2.65	871	0.2	2.71	290	1.3	3.74	347	0.61
5 components	3.6	2.31	475	1.6	2.59	333	0.2	2.71	290	1.3	3.75	344	0.79
				1.6	2.70	333							
5 components	3.6	2.31	482	1.6	2.60	355	0.2	2.71	290	1.3	3.74	469	0.57
				1.6	2.71	548							
Resting (P/M)													
4 components	3.6	2.31	599	3.2	2.63	634	0.2	2.71	295	1.3	3.73	361	0.72
5 components	3.6	2.31	582	1.6	2.58	333	0.2	2.71	295	1.3	3.74	392	0.84
				1.6	2.67	333							
5 components	3.6	2.31	566	1.6	2.60	376	0.2	2.71	295	1.3	3.74	360	0.69
				1.6	2.68	538							
Reduced (P/M^{-})													
4 components	3.6	2.33	578	3.2	2.60	938	0.2	2.66	398	1.3	3.72	245	0.19
5 components	3.6	2.33	655	1.6	2.54	333	0.2	2.66	398	1.3	3.72	243	0.25
				1.6	2.66	333							
5 components	3.6	2.33	632	1.6	2.54	479	0.2	2.66	398	1.3	3.72	251	0.17
				1.6	2.66	534							

[a] F is defined by $\sum_i(\chi_{exp} - \chi_{calc})^2 \cdot k^6/\text{npts}$. [b] $\Delta E_0 = -3$ eV. [c] $\Delta E_0 = -8$ eV. [d] $\Delta E_0 = -6$ eV. [e] $\Delta E_0 = -10$ eV.

constructed by constraining all similar Fe−S and Fe−Fe distances to the same value. The largest multiple scattering contribution found for the M-center was a 3.6 Å Fe−S−Fe path (the distance refers to the total path length divided by 2) that was only 7% of the largest Fe−S interaction at ~2.3 Å and ~25% of the 3.7 Å single-scattering Fe−Fe interaction. Examination of P-cluster multiple scattering is complicated by the current discrepancy between the crystal models.[4-6] Although examination of the core 4Fe−4S cube structures does not show any multiple scattering in the <3 Å region, the possibility of multiple scattering in the >3 Å range is strongly dependent on the overall symmetry within the cubes and their bridging geometry. The Mo EXAFS data was also checked for multiple scattering. Although significant multiple scattering paths for the histidine and homocitrate ligand groups were found, their contributions are also not important in the range below ~3 Å used for the current analysis.

The average Fe−Fe distance of 2.65 Å is not significantly different from the 2.63 Å value for resting enzyme. However, an important result from the four-shell IDS fit is the large σ value of ~0.09 Å for the 2.65 Å Fe−Fe interaction. Typical values for thermal motion disorder of short bridged metal−metal distances are on the order of 0.05 Å or less, so a σ of ~0.09 Å indicates a measure of "static" as opposed to "thermal" disorder. One interpretation is that upon oxidation, all Fe−Fe distances in nitrogenase become more disordered, with the

average value at 2.65 Å. A simple alternative is that the P-cluster Fe−Fe interactions have all expanded, while the cofactor interactions have remained the same, so as to give an overall average of 2.65 Å.

Examination of the radial distribution function derived from the resting nitrogenase crystal structure[5,6] suggests dividing the short Fe−Fe interactions into two subgroups, one with an average Fe−Fe coordination number $N = 1.6$, accounting for Fe−Fe interactions in the M center, and another with $N = 1.6$ corresponding to Fe−Fe interactions in the P-cluster. Splitting the radial distribution is also chemically reasonable, since the three-coordinate Fe in the M center might be expected to have stronger Fe−Fe bonding interactions and significantly shorter distances. Previous EXAFS analyses of isolated FeMo-cofactor also found relatively shorter average Fe−Fe distances than for the intact protein.[11b]

With the current range of data, using the resolution criterion that $\Delta R \cong \pi/2\Delta k$,[27] we cannot truly resolve backscatterers that have similar atomic numbers and that have distances that differ by less than 0.14 Å. We nevertheless explored a simple "split-shell" model, allowing for two different short Fe−Fe components, while constraining as many other parameters as possible. Although the fit did not improve if the σ_{Fe-Fe} values were constrained at 0.057 Å (the value found for the $[Fe_6S_6Cl_6]^{3-}$ prismane complex),[25] the fit did improve somewhat with unconstrained σ_{Fe-Fe} values (Table 1). The constrained five component fit (Table 1) found short Fe−Fe interactions at 2.59 and 2.70 Å. Although part of the improvement is expected because of the additional degrees of freedom introduced by the new interaction, the distances are chemically reasonable. With 15 different types of Fe in nitrogenase, the true radial distribution is no doubt more complex than this simple model.

The previously reported[9] resting enzyme and thionin-oxidized enzyme Fe EXAFS were reinterpreted with the new model (Table 1). As expected, the thionin-oxidized spectrum, which produced the largest σ_{Fe-Fe} values in the four-shell fits, gave the largest difference in Fe−Fe distances when fit with the split-shell model, with an average M-center short Fe−Fe of 2.61 Å, compared to a P-cluster short Fe−Fe of 2.74 Å. The 2.74 Å Fe−Fe distance is the same as that seen in a synthetic Fe_4S_4 cluster,[28] while the 2.61 Å distance compares favorably with the 2.64 Å value reported for isolated FeMo-co.[11] Split-shell analysis of the resting enzyme Fe EXAFS also gave a relatively short M center Fe−Fe distance of 2.58 Å and a P-cluster average of 2.67 Å, compared to respective crystallographic values (at room temperature) of 2.60 and 2.71 Å. As noted by others, the M-center distances are near the bond length range for Fe−Fe bonds.[29]

Singly Reduced MoFe Protein. Mo and Fe EXAFS spectra and Fourier transforms, illustrating the extraction process for obtaining the reduced E_1 spectra, are shown in Figure 3. The noise level for the pure E_1 spectrum is increased; this is expected for a spectral subtraction, and the contribution from the ±2.5 % error in the $E_0 + E_1$ is small enough to be neglected in the subtraction. To provide additional constraints for the more complex Fe analysis, we first fit the Mo EXAFS data. The Mo EXAFS Fourier transform was filtered to select the region from 1−3 Å and backtransformed. The fits yielded Mo−(O,N), Mo−S, and Mo−Fe distances of 2.13, 2.36, and 2.65 Å, respectively (Table 2). Of these distances, the most significant

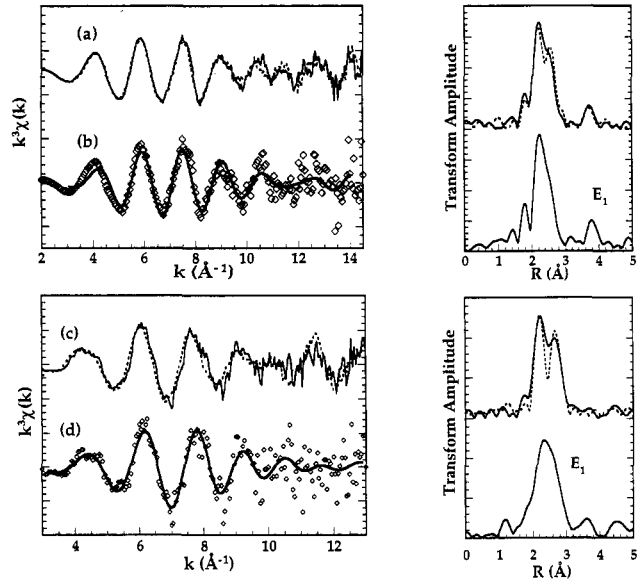

Figure 3. (a) Fe EXAFS of the $E_0 + E_1$ mixture overlayed with the resting protein EXAFS (dashed). (b) Result of subtraction shown with individual data points and the resulting filtered EXAFS. (c) Mo EXAFS of the $E_0 + E_1$ mixture overlayed with the resting protein EXAFS (dashed). (d) Result of subtraction shown with individual data points and the resulting filtered EXAFS. The Fourier transforms for the corresponding EXAFS are shown on the right.

result is the apparent 0.06 Å contraction in the Mo−Fe distance. This Mo−Fe distance and the associated σ of 0.063 Å were then used as constraints in the analysis of the Fe EXAFS of the E_1 enzyme (P/M^-).

For the Fe EXAFS of E_1, the dominant transform feature is still the ~2.3 Å Fe−S interaction. The 2.7 Å (Fe−Fe plus Fe−Mo) peak that is resolved in the E_0 transform is only a shoulder in the $E_0 + E_1$ mixture, becoming even less visible in the pure E_1 transform. However, in the 3−5 Å region, the Fe−Fe interaction at ~3.75 Å from cross-cluster cofactor interactions is still obvious in the pure E_1 spectrum, which helps maintain confidence in the subtraction procedure.

To help limit the number of free parameters in the curve fitting analysis, two regions were filtered from the initial Fe EXAFS Fourier transform, an inner shell region from ~1−3.5 Å and an outer shell from 3.2−4.5 Å. For the shorter distance region, we conducted the same kind of single Fe−Fe shell and split Fe−Fe shell analyses described for the IDS oxidized protein, but now fixing the Fe−Mo distance and σ at the 2.65 Å and 0.063 Å values from the Mo EXAFS on E_1. The results are summarized in Table 1 and Figure 4. Using a single short Fe−Fe interaction, we found Fe−S and Fe−Fe distances of 2.33 and 2.60 Å, respectively. Allowing for a split Fe−Fe distribution gave subshell average distances of 2.54 and 2.66 Å. The outer shell fit to an Fe−Fe interaction at 3.72 Å is only slightly shorter than the 3.74 Å distance seen in resting enzyme. In order to truly determine the presence of long range structural changes within the M-center, an examination of the ~5 Å Mo−Fe distance previously reported[10b] would be valuable. Unfortunately, this distance was seen in single crystal nitrogenase samples oriented in such a way as to optimize this interaction. With the concentrations presently available for these reduced samples and the noise introduced by the subtraction, an observation of this interaction is unlikely at this time.

The overall trends observed between four different oxidation levels of the nitrogenase Mo−Fe protein are summarized in Figure 5. Many of the individual changes are on the order of typical EXAFS error bars, which are generally considered ±0.02

(27) Lee, P. A.; Citrin, P. H.; Eisenberger, P.; Kincaid, B. M. *Rev. Mod. Phys.* **1981**, *53*, 769−806.
(28) Laskowski, E. J. Frankel, R. B.; Gillum, W. O.; Papaefthymiou, J. R.; Ibers, J. A.; Holm, R. H. *J. Am. Chem. Soc.* **1978**, *100*, 5322−5337.
(29) Gonzalez-Moraga, G. *Cluster Chemistry*; Springer-Verlag: Berlin, 1993.

Table 2. *Azotobacter vinelandii* Nitrogenase Mo K-Edge EXAFS Fitting

	Mo−O/N[b]			Mo−S[c]			Mo−Fe[d]			
	N	*R*, Å	$\sigma^2 \times 10^{-5}$, Å^2	*N*	*R*, Å	$\sigma^2 \times 10^{-5}$, Å^2	*N*	*R*, Å	$\sigma^2 \times 10^{-5}$, Å^2	[a]*F*
thionine oxidized (P^{2+}/M^+)	3.0	2.17	317	3.0	2.38	399	3.0	2.72	435	0.51
resting (P/M)	3.0	2.20	283	3.0	2.36	340	3.0	2.71	310	0.87
reduced (P/M^-)	3.0	2.13	263	3.0	2.36	178	3.0	2.65	397	0.54

[a] *F* is defined by $\Sigma|\chi_{exp} - \chi_{calc}|$/npts. [b] $\Delta E_0 = 3.3$ eV. [c] $\Delta E_0 = -14$ eV. [d] $\Delta E_0 = -10$ eV.

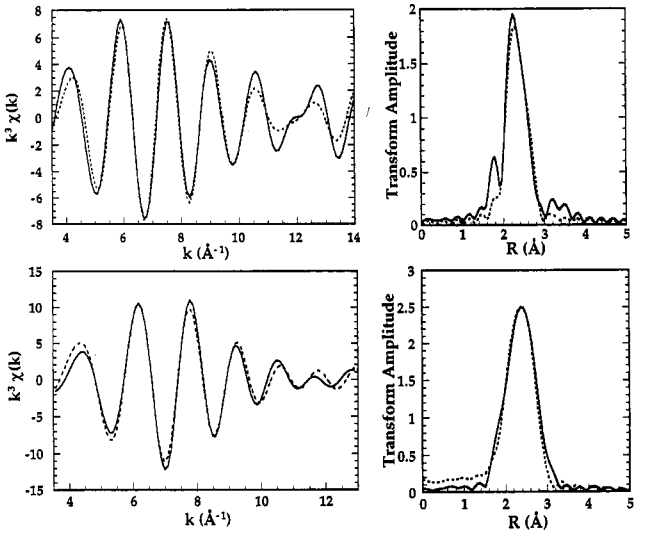

Figure 4. *Top:* Fe EXAFS and Fourier transform for the filtered data (shown solid) and the fit (shown dashed). *Bottom:* Mo EXAFS of the filtered data (shown solid) and resulting fit (shown dashed).

Å for simple, well-behaved systems.[30] Still, meta-analysis of the overall data reveals two clear trends: a contraction of the calculated metal−metal distances as the enzyme becomes more reduced and an expansion in the Fe−S distances.

We have illustrated the degree of M-center "breathing" between oxidized and reduced forms, implied by the EXAFS analysis, by constructing a symmetrized model based on the crystallographic geometry (Figure 6). Of course, there is no reason for all the M center short Fe−Fe distances to be the same, and the structure in the protein may be distorted from this idealized picture. For example, the central iron cage could elongate or flatten, and one possible distortion that is consistent with the EXAFS is also illustrated.

Since the publication of a crystallographic model for the MoFe protein, much attention has been paid to location of possible N_2 binding sites; this is essential to understanding the mechanism of enzymatic activity. The current model can be thought of as creating a sort of "cage" created by the central 6 Fe. In the resting structure, this cage is ~0.5 Å too small for N_2 to enter, so it has been suggested that the cluster breaks open to accommodate dinitrogen.[31] Deng and Hoffman have considered the expansion of the cage required to accommodate an interior N_2; they suggest that the Fe−Fe distances would have to expand to ~3.0 Å.[32] They and others have also considered binding sites on the outer surface of the cage.[5,32,33]

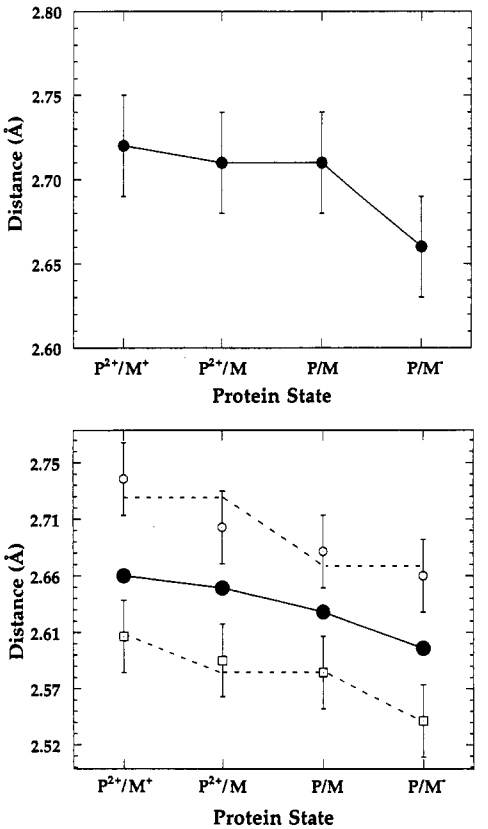

Figure 5. The trends in metal−metal distances during protein reduction/oxidation. *Top:* Trend in the Fe−Mo distance for different redox states of the MoFe protein. *Bottom*: The center plot (solid) shows the trend in the Fe−Fe distance for the four-component fits, while the two outer plots show the expected trend (dashed) and actual EXAFS distances (open circles, open squares) from the five-component fits. The expected trend line was generated based on the assumption that the P-cluster is in one state for the IDS and thionine samples, while it is in a different state for the resting and reduced samples. Similarly, the M-center should be the same for both IDS oxidized and resting samples, yet enter different states upon oxidation or reduction.

Our data, ranging from thionin-oxidized (three-electron oxidized per $\alpha\beta$ subunit) to the E_1 form (one electron reduced), show that, at least over this range of reduction, the average Fe−Fe distance seen by EXAFS does not expand, rather it contracts slightly.

The significance of the current results can be interpreted in two different ways. On the one hand, the general similarity of all of the Mo and Fe EXAFS for oxidized and reduced nitrogenase suggests that profound transformations have not occurred. For example, the persistence of the long cross-cluster 3.75 Å Fe−Fe peak in all of the Fe EXAFS Fourier transforms suggests that these interactions, and hence the overall M center structures, are similar in resting, oxidized, and one-electron reduced forms. Although this result is not very surprising, rearrangements were certainly possible. There are numerous examples of clusters which rearrange their polyhedral geometries

(30) *X-Ray Absorption: Principles, Applications, Techniques of EXAFS, SEXAFS and XANES*; Prins, R., Königsberger, D., Eds.; Wiley: New York, 1988.

(31) (a) Schrauzer, G. N.; Docemeny, P. A.; Palmer, J. G. *Z. Naturforsch. Sect. B-A J. Chem. Sci.* **1993**, *48*, 1295−1298. (b) Schrauzer, G. N. *J. Inorg. Biochem.* **1993**, *51*, 370.

(32) Deng, H.; Hoffman, R. *Angew. Chem., Int. Ed. Engl.* **1993**, *32*, 1062−1065.

(33) Dance, I. G. *Aust. J. Chem.* **1994**, *47*, 979−990.

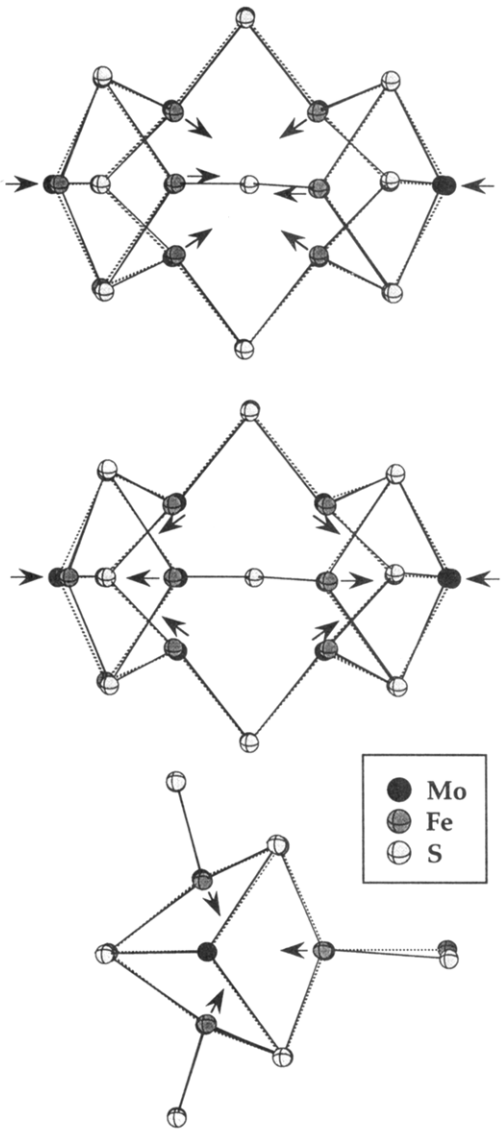

Figure 6. Two possible structural rearrangements of the M-center in the singly reduced state using the EXAFS distances for thionine oxidized and singly reduced MoFe protein. *Top*: The most symmetric case, where all Fe−Fe distances in the M-center contract. *Middle*: A possible rearrangement where the central portion of the cluster expands, while the ends of the M-center contract in such a way that the overall average Fe−Fe distance is shorter. *Bottom*: An end on view of the rearrangement shown in the top figure, further showing the contraction of the cluster. Although the bottom figure was calculated for the symmetric rearrangement (top), it is consistent with both models shown.

upon electron transfer.[34] The potential influence of valence electrons on the molecular geometry of clusters has been appreciated for more than 30 years.[35]

The ~0.07 Å contractions proposed for Fe−Fe distances between thionin-oxidized and one-electron reduced forms are chemically reasonable in magnitude. For example, a 0.06 Å contraction with "change of electron count" occurs when $S_2Ni_3(C_5H_5)_3$, with a mean Ni−Ni distance of 2.80 Å,[36] is oxidized to the recently isolated monocation,[37] and a further contraction to 2.53 Å occurs in $(C_5H_5)_3Ni_3(CO)_2$, with four fewer electrons for Ni−Ni interactions from the original cluster.[38] Another example of shortening on removal of an electron is the complex $SFeCo_2(CO)_9$,[39] where the average metal−metal distance is 0.08 Å shorter than the 2.64 Å distance in $SCo_3(CO)_9$.[35] These changes can be rationalized by an electron counting scheme formulated by Lauher for trinuclear clusters that considers the highest 3 of the 27 molecular orbitals formed from the metal atomic orbitals as antibonding.[40]

Instead of expanding, metal−metal distances do sometimes contract with addition of electrons. For example, in aqueous Mo chemistry, the Mo−Mo distances shorten from ~2.6 Å for Mo(V)−Mo(V) dimers to ~2.5 Å in the Mo(IV) trimer all the way to 2.12 Å in the Mo(II) dimer.[41] However, most such examples occur for early transition metals which are initially lacking sufficient d-electrons for multiple metal−metal bonding. The contraction we observe in Fe−Fe and Mo−Fe distances upon reduction is thus surprising and perhaps important. Both in $[Fe_4S_4]^{n+}$ clusters, where $n = 1, 2, 3$, and in $[Fe_6S_6L_6]^{n-}$ prismanes, where $n = 2, 3$, addition of electrons results in expansion of the Fe−Fe distances.[42] Also, in the $[Fe_6S_6L_6(Mo(CO)_3)_2]^{n-}$ capped prismanes where $n = 2, 3$, the more reduced species has longer Mo−S and Mo−Fe distances.[25]

Since the majority of documented metal clusters expand as electrons are added, the observed contraction in EXAFS average distances begs for some explanation. The clusters certainly catalyze special chemistry, so there could be something special about the bonding of the three-coordinate Fe centers in the M center cage. There is one alternative explanation that we cannot yet refute, related to EXAFS artifacts from asymmetric distribution functions. Eisenberger and Brown observed an anomalous apparent contraction with increasing temperature in Zn metal EXAFS.[43] They found that in the case of an asymmetric distribution function that tails to longer distances, the EXAFS is disproportionately sensitive to the sharp leading edge of the distribution and yields distances shorter than the arithmetic average. The same effect might occur for particular distortions of the M center and P cluster. For example, if the M center expanded along its 3-fold axis, while contracting for two of the Fe−Fe distances in the planes perpendicular to the long axis, a broad asymmetric distribution could be created. Calculations performed by Deng and Hoffman indicate the possibility of asymmetry where the MoFeS fragment of the M-center may exhibit a contraction, while the FeS end of the M-center may undergo a small expansion.[44]

Asymmetrical structural changes are well documented not only for biological $[Fe_4S_4]$ clusters and their models but also in other small molecules such as the $[\{Fe(\mu_3\text{-}S)Cp\}_4]$ series.[34c] The neutral cluster has two short (2.64 Å) and four long (3.36 Å) Fe−Fe distances,[45] going to two short (2.64 Å), two medium (3.19 Å), and two long (3.32 Å) Fe−Fe distances upon one-

(34) (a) Rieck, D. F.; Rae, A. D.; Dahl, L. F. *J. Chem. Soc. Chem. Comm.* **1993**, 585−587. (b) Drake, S. R.; Barley, M. H.; Johnson, B. F. G.; Lewis, J. *Organometallics* **1988**, *7*, 806−812, and references cited therein. (c) Geiger, W. E.; Connelly, N. G. *Adv. Organomet. Chem.* **1985**, *24*, 87−130, and references cited therein. (d) Geiger, W. E. *Prog. Inorg. Chem.* **1985**, *33*, 275, and references cited therein.

(35) Wei, C. H.; Dahl, L. F. *Inorg. Chem.* **1965**, *4*, 493−499.

(36) Vahrenkamp, H.; Uchtman, V. A.; Dahl, L. F. *J. Am. Chem. Soc.* **1968**, *90*, 3272−3273.

(37) North, T. E.; Thoden, J. B.; Spencer, B.; Dahl, L. F. *Organometallics* **1993**, *12*, 1299−1313.

(38) Maj, J. J.; Rae, A. D.; Dahl, L. F. *J. Am. Chem. Soc.* **1982**, *104*, 3054.

(39) Hock, A.; Mills, O. S. *Advances in the Chemistry of Coordination Compounds*; The Macmillan Co.: New York, 1961.

(40) Lauher, J. W. *J. Am. Chem. Soc.* **1978**, *100*, 5305−5315.

(41) Cramer, S. P.; Gray, H. B.; Dori, Z.; Bino, A. *J. Am. Chem. Soc.* **1979**, *101*, 2770−2772.

(42) Stiefel, E. I.; George, G. N. in *Bioinorganic Chemistry*, Bertini, I., Gray, H. B., Lippard, S. J., Valentine, J. S., Eds.; University Science: Mill Valley, CA; 1994; pp 365−453, and references cited therein.

(43) Eisenberger, P.; Brown, G. S. *Solid State Comm.* **1979**, *29*, 481−484.

(44) Deng, H.; Hoffman, R. Personal communication.

(45) (a) Schunn, R. A.; Fritchie, C. J.; Prewitt, C. T. *Inorg. Chem.* **1966**, *5*, 892. (b) Wei, C. H.; Wilkes, G. R.; Treichel, P. M.; Dahl, L. F. *Inorg. Chem.* **1966**, *5*, 900.

electron oxidation[46] and four short (2.83 Å) and two long (3.25 Å) Fe−Fe distances with the next oxidation.[47] Thus, although the cluster volume and average Fe−Fe distance expands with reduction, the leading edge of the Fe−Fe distribution function actually moves to shorter distances. Relevant to possible distortions in hexanuclear clusters, we note that in $Co_6C(CO)_{12}S_2$, the Co−Co distances along the long axis of the trigonal prism are 2.67 Å compared to the 2.44 Å distances in the planes perpendicular to the long axis.[48] In the $[Fe_6C(CO)_{16}]^{2-}$ complex, the short Fe−Fe distances range from 2.55 to 2.72.[49] The shortest metal−metal vectors in both cases are perpendicular to the approximate 3-fold axes. In this spirit, we again divided the Fe−Fe component for the reduced Fe EXAFS (P/M^-) and found distances of 2.56 Å ($N = 1.1$, $\sigma^2 = 0.00263$ Å^2), 2.66 Å ($N = 1.6$, $\sigma^2 = 0.00311$ Å^2) and 2.84 Å ($N = 0.5$, $\sigma^2 = 0.00115$ Å^2) with a factor of 2 improvement in the quality of fit value. Although there are far too many variables for this type of fit to be definitive, it does help to illustrate that there are many possible distortions that may be masked within our resolution limits.

Whether or not the especially short Fe−Fe distances represent arithmetic averages, it is clear that at least some of the Fe−Fe distances are especially short. The proposed reduced M-center value of 2.54 Å (a 0.04 Å contraction from the resting protein) is similar to Fe−Fe distances in clusters with Fe−Fe bonding. The Fe−Fe distances proposed for the M-center are close to the 2.52 Å interaction in $Fe_2(CO)_9$, where metal−metal bonding has been proposed[50] (or denied[51]). There is also a strong analogy with the cluster $S_2Fe_3(CO)_9$[35] which contains Fe−Fe distances of 2.59 (av) and 3.37 Å.

The possible expansion of the P-cluster upon oxidation may also be significant, but the lower symmetry makes it difficult to model. For the IDS oxidized MoFe protein, for which only the P-cluster changes oxidation state, we observed an expansion of the overall average short Fe−Fe distance from 2.62 to 2.65 Å. Using the split-shell model (although the data does not allow unambiguous resolution of P-cluster and M-center distances), one interpretation is that the average P-cluster Fe−Fe distance expands from ~2.67 to ~2.72 Å (these numbers are arrived at by taking the average distances from the thionine and IDS oxidized results and the average of resting and reduced results). Recent crystallographic modeling of the MoFe protein has also indicated that, when exposed to agents capable of oxidizing P-clusters, there is an expansion in the average Fe−Fe distances in the P-cluster.[52]

Summary

The metal clusters in nitrogenase "breathe" slightly upon reduction or oxidation. Contrary to expectations, a significant fraction of the average Fe−Fe distances contract as the enzyme becomes more reduced. Comparison with known cluster model compounds suggests that rearrangement during further reduction of the enzyme may be significant and deserves additional study.

Acknowledgment. The authors wish to thank M. M. Grush for help in data acquisition and scientific discussion. Support from the Department of Energy, Office of Health and Environmental Research and the Department of Agriculture through Grants DOA-91-37305-6514 (to S.P.C.) and DOA-94-03945 (to B.J.H.) as well as NIH grant GM-33965 (to B.J.H.) is gratefully acknowledged. The National Synchrotron Light Source is supported by the Department of Energy, Division of Materials Sciences and Division of Chemical Sciences. The Stanford Synchrotron Radiation Laboratory is supported by the Department of Energy, Office of Basic Energy Sciences.

JA9516569

(46) Toan, T.; Fehlhammer, W. P.; Dahl, L. F. *J. Am. Chem. Soc.* **1977**, *99*, 400−407.

(47) Toan, T.; Teo, B. K.; Ferguson, J. A.; Meyer, T. J.; Dahl, L. F. *J. Am. Chem. Soc.* **1977**, *99*, 408−416.

(48) Bor, G.; Gervasio, G.; Rossetti, R.; Stanghellini, P. L. *J. Chem. Soc., Chem. Commun.* **1978**, 841−843.

(49) Baird, N. C.; West, R. M. *J. Am. Chem. Soc.* **1971**, *93*, 3073−3074.

(50) (a) Barnett, B. L.; Krüger, C. *Angew. Chem., Int. Ed. Engl.* **1971**, *10*, 910−911. Mealli, C.; Prosperio, D. M. *J. Organomet. Chem.* **1990**, *386*, 203−28.

(51) Reinhold, J.; Hunstock, E. *New. J. Chem.* **1994**, *18*, 465−471.

(52) Bolin, J. Personal communication.